

Evaluation of Radiation Damaged P-in-n and N-in-n Silicon Microstrip Detectors

Y. Unno¹, T. Yamashita⁵, S. Terada¹, T. Kohriki¹, G. Moorhead², Y. Iwata³, R. Takashima⁴, M. Ikeda³, E. Kitayama⁵, K. Sato³, T. Kondo¹, T. Ohsugi³, I. Nakano⁵, C. Fukunaga⁶, P.W. Phillips⁷, D. Robinson⁸, L.G. Johansen⁹, P. Riedler¹⁰, S. Roe¹⁰, S. Stapnes¹¹, and B. Stugu⁹

¹Institute of Particle and Nuclear Studies, High Energy Accelerator Research Organisation (KEK), Tsukuba 305-0801, Japan

²School of Physics, University of Melbourne, Parkville, Victoria 3052, Australia

³Physics department, Hiroshima University, Higashi-Hiroshima 739-8526, Japan

⁴Education department, Kyoto University of Education, Kyoto 612-0863, Japan

⁵Physics department, Okayama University, Okayama 700-8530, Japan

⁶Physics department, Tokyo Metropolitan University, Hachiohji 192-0397, Japan

⁷Particle Physics department, Rutherford Appleton Laboratory, Chilton, Didcot, Oxon OX11 0QX, UK

⁸Cavendish laboratory, University of Cambridge, Cambridge CB3 0HE, UK

⁹Department of Physics, University of Bergen, N-5007 Bergen, Norway

¹⁰PPE, CERN, CH-1211 Geneve 23, Switzerland

¹¹Department of Physics, University of Oslo, N-0316 Oslo 3, Norway

Abstract

Two p-in-n and one n-in-n silicon microstrip detectors were radiation-damaged and beamtested. Comparison was made for the p-in-n and the n-in-n in high resistivity wafers, and the p-in-n in a low and a high resistivity wafer. The charge collection showed a clear difference in the n-in-n and the p-in-n detectors, which suggested that the charge signals were split into strips in the p-in-n detectors. Although a difference of the low and the high resistivity wafers was observed in the body capacitance measurement, little difference was observed in the beamtest results.

I. INTRODUCTION

In the high energy hadron colliders, such as LHC, the number of particles generated at the interaction point is so large that the detectors installed near the interaction point need to be radiation-tolerant. The silicon microstrip detectors in the ATLAS detector will experience the fluence of particles of 3×10^{14} particles/cm² over the 10 years of operation [1]. Radiation-tolerant design has been developed including the development of structures sustaining higher bias voltages and improvement in reducing the high electric field in the edges of implantation [2]. Developed radiation-tolerant silicon strip detectors has been evaluated, starting from the double-sided detector [3], and then the single-sided detectors with n-strip readout [4].

One of the major radiation damage to the Silicon detectors is the mutation of the bulk type from the initial n-type to the p-type due to the creation of effective acceptor states in the bulk. Single-sided detector with n-strip readout was efficient below full-depletion because the p-n junction was in the n-strip side after the type-inversion. The detector, however, required double-sided processing in fabrication to make the initial p-n junction in the backside.

The p-readout was not considered first because of two reasons: (1) it may require full-depletion to be efficient, and (2) it may not sustain high bias voltages. The second point needs an explanation. The p-readout single-sided silicon strip detector sustains the bias voltage in the p-n junction at the edge of p-

strips and the p-bias ring surrounding the p-strips, in the initial state. The backside is a planar densely-doped n-layer (n^+). When the detector was sawed out, the interface of the planar n^+ and the silicon bulk was on the surface of the cutting edge. When the bulk type is inverted, the interface becomes the p-n junction. In the non-radiation-damaged detectors, the p-n junction on the surface of the cutting edge is known to break even with a small bias voltage.

Recent experience in the study of the radiation tolerant silicon strip detectors, the interface of the planar n^+ and the inverted p-bulk did not break in a low bias voltage, not even as high as several hundred volts. With the development of sustaining high bias voltages and the accumulation of knowledge of the charge collection in the p-strips in the radiation-damaged detectors, e.g., the p-side of the double-sided detector, it was becoming likely that the improved p-readout single-sided detector would work sufficiently for the application in the ATLAS experiment. The p-readout in the n-bulk silicon detectors had cost-advantage because of the simple backside processing.

Other interesting issue in the bulk damage was the increase of the depletion voltage in the different resistivity wafers. The common resistivity of wafers of the silicon microstrip detectors had been 4 to 8 k Ω cm, so-called “high resistivity” wafers. The low resistivity wafers, e.g., 1 k Ω cm, had more donors. The radiation damage would create effective acceptors, and, if the donors were to remain, the donors would help to reduce the depletion voltage after the type-inversion. Although there was a report that the donors were removed at low fluences [5], it was important to confirm the result.

In this report, three silicon microstrip detectors were put in the tests: one with p-readout in a high resistivity n-bulk wafer (p-in-n high), one with p-readout in a low resistivity n-bulk wafer (p-in-n low), and one with n-readout in a high resistivity n-bulk wafer (n-in-n high). These detectors were radiation-damaged with protons and then subsequently put in a beamtest to evaluate the charge collection in the detectors.

II. DETECTOR SAMPLES

The p-in-n and n-in-n silicon microstrip detectors were fabricated along with the ATLAS silicon microstrip detector specification [1]. One p-in-n detector (Sintef p-in-n: SinP10) [6] and one n-in-n detector (Ham n-in-n: HamN) [7] were made on high resistivity n-bulk wafers, 5 k Ω cm and 4 k Ω cm, respectively. One p-in-n detector was made on a low resistivity wafer, 1 k Ω cm (Ham p-in-n: HamP) [7].

The detectors had a strip pitch of 80 μ m and an outer dimension of 63.6 mm (width) x 64.0 mm (strip direction). The detector's parameters are summarized in Table 1. The nominal thickness of the detectors was 300 μ m. The measured thickness were 293 μ m, 300 μ m, and 300 μ m, for the Sintef p-in-n, the Ham p-in-n, and the Ham n-in-n detector, respectively, with a measurement error of 1 μ m order.

Table 1.
Parameters of the p-in-n and n-in-n silicon strip detectors

Detector type:	AC-coupled, Single-sided
Bulk:	N-bulk, nominal 300 μ m thickness
Resistivity:	High (4 or 5 k Ω cm) and Low (1k Ω cm)
Size (Outer):	6.36 cm \times 6.4cm (width \times length)
Strip area:	Width: 770 strips \times 80 μ m = 61.6 mm
Backside:	Uniformly doped n ⁺ layer
Strip parameters:	
Length:	62 mm
Strip pitch:	80 μ m
Implant width:	16 μ m
Resistance of implant:	≤ 100 k Ω /cm
Readout pitch:	80 μ m
AC coupling:	SiO ₂ + SiN
Width of Al. readout:	16 μ m
Resistance of Al. readout:	≤ 20 Ω /cm
Bias resistance:	1.5 \pm 0.5 M Ω

III. PROTON IRRADIATION

A. Irradiation at KEK

The detectors were radiation-damaged with the 12 GeV protons in the EP1A beamline of the 12 GeV Proton Synchrotron at KEK [8]. The irradiation used the setup being developed for irradiations in the past [9]. The thermo-box stored the detectors and kept the temperature inside at -5 $^{\circ}$ C in average.

The nominal beam size was 61 mm full-width-half-maximum (FWHM) in horizontal and 26 mm FWHM in vertical. In order to cover the 6 cm x 6 cm detector area uniformly, the thermo-box was moved. The total intensity was counted with a secondary emission chamber (SEC) and triggered the stage movement. The absolute fluence was estimated from the activation of 1 cm x 1 cm Aluminium foils in 5 x 5 matrix attached at the detector position.

In the run, there was a change of beam size, which invalidated our calculation of the uniformity. With a correction to the

movement, we could only achieve the fluence uniformity of $\pm 16\%$ at the maximum and the minimum relative to the average in the readout region. The fluence variation in positions is shown in Figure 1. At the centre of the detector, the fluence was 4.2×10^{14} protons/cm², with an error of 10% which was dominated by the error of the cross section. In the subsequent beamtest, the readout region was set in the middle of the detector with an area of 2 cm x 2 cm horizontally and vertically. The detectors were kept cold, at -5 $^{\circ}$ C in average in the beamline, and stored at 0 $^{\circ}$ C after extraction.

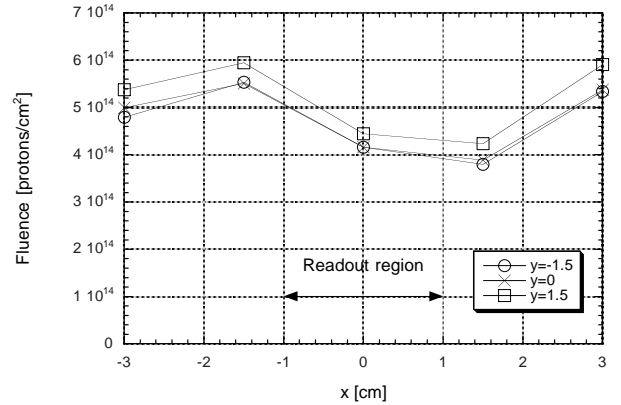


Figure 1: Proton fluence in the detector. The horizontal axis, x, is the position across the strips, the direction of the width, and the parameter, y, is the position along the strip, the direction of the length, in the unit of cm.

Before the beamtest, the radiation-damaged detectors were warmed up, for 5 days in the room temperature because of the beamtest preparation and for 7 days at 28 $^{\circ}$ C, in order to anneal the damage and to include the warm-up for maintenance in the real experiment. The full-depletion voltage would have increased by about 20% above the minimum full-depletion voltage.

The annealing and the anti-annealing of the full-depletion voltage was experimentally parameterized by H. Ziock [10]. Because of the different time-dependence of the annealing and the anti-annealing effects, the full-depletion voltage first decreases and then increases. The change of the full-depletion voltage in time can be expressed by scaling the time with the characteristic time to reach the minimum, the time of minima. The temperature dependence of the time of minima is shown in the bottom figure of Figure 2 and the full-depletion voltage at a fluence of 1×10^{14} p/cm² is shown in the top figure of Figure 2. The full-depletion voltage is parameterized to be linear to the fluence.

B. Capacitance measurement

After the warm-up, the body capacitance, i.e., the capacitance between the top and the bottom surface, was measured as a function of bias voltage. This was a common method to estimate the full-depletion voltage from the corner of the theoreti-

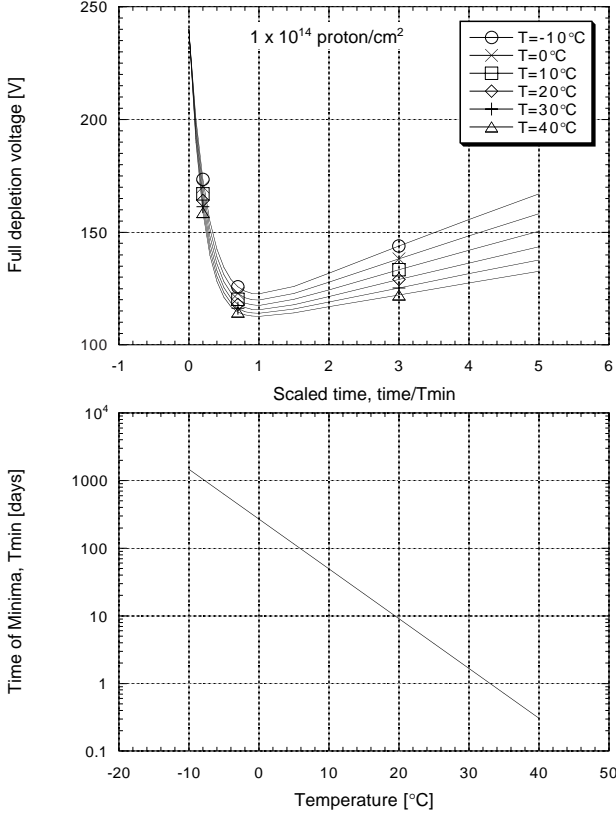


Figure 2: Expected full-depletion voltage as parameterized by H. Zioka as a function of time scaled by the time of minima (top figure), and the temperature dependence of the time of minima (bottom figure)

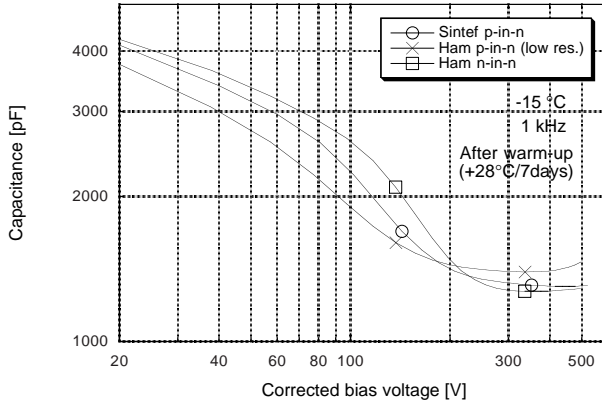


Figure 3: Body capacitances of the radiation-damaged detectors as a function of the bias voltage after the warm-up. Sintef p-in-n (circle), and Hamamatsu n-in-n (square) were in the high resistivity bulk, and Hamamatsu p-in-n (cross) was in the low resistivity bulk wafer.

cal $V^{-0.5}$ falling-off and the saturation, where V was the bias

voltage. The environment temperature in the measurement was set at -15°C in order to limit the leakage current. The measured capacitances are shown in Figure 3.

The first impression was that the detector in the low resistivity wafer, HamP, had the lowest corner voltage, the p-in-n detector in the high resistivity wafer, SinP, the second, and the n-in-n in the high resistivity, HamN, the highest. This may suggest: the low resistivity wafer would develop lower full-depletion voltage than the high resistivity ones, and the p-n junction in strip geometry (radiation-damaged n-in-n detector) would require more voltages in depleting the bulk than the p-n junction in planar one (radiation-damaged p-in-n).

However, as evident from the data, (1) the falling-off of the capacitance was not monotonic and did not follow the theoretical expectation of $V^{-0.5}$, (2) the corner of the falling-off and the saturation was very mild, and (3) the order of the saturated capacitances was opposite to the order of the capacitances in the falling-off. Because of these observations, it was difficult to draw the corner voltage and, in turn, the full-depletion voltage.

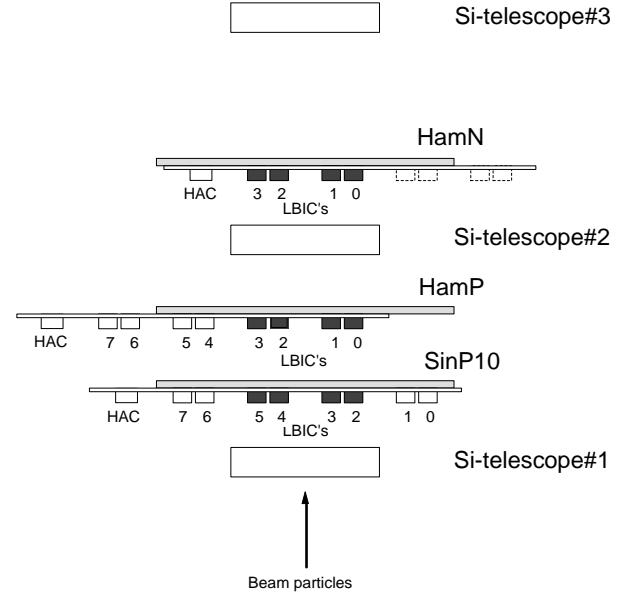


Figure 4: Beamtest setup of the radiation-damaged detectors with the silicon strip detector telescopes which define the beam particle positions. The distance between each detector was about 30 mm.

IV. BEAMTEST

A. Setup

The radiation-damaged detectors were beamtested at the $\pi 2$ beamline of the 12 GeV proton synchrotron at KEK [11]. The negatively charged pi-mesons of 3 GeV/c were selected. The detectors were positioned in a thermo-box in the beamline as shown in Figure 4, together with the “Si-telescopes”.

Each detector was connected to a readout hybrid which carried a fast-shaping on-off readout electronics (binary readout)

with the 64 channel Bipolar amp-shaper-discriminator LSI chips (LBIC) and the 128 channel CMOS digital buffer LSI chips (CDP) [12]. The readout was interfaced with a communication chip, HAC, on the hybrid to the backend electronics and the data acquisition system. Because of limited available chips, only 4 LBIC's areas were readout in the middle of the detectors.

The radiation-damaged detectors were sandwiched with silicon strip detectors with a Viking chips [13], "Si-telescopes", which provided a position resolution of 5 μm of the incident particles. The detectors were separated by about 30 mm. The smearing by the multiplescattering was less than 10 μm when the incident particle positions at the detectors were interpolated with the Si-telescopes [14].

B. Leakage currents

The inside environment of the thermo-box was kept at -17°C in order to keep the leakage current small and not to introduce the thermal runaway in the detector at the highest bias voltage. The leakage current was monitored during the beamtest. A typical bias voltage dependence is shown in Figure 5.

All three detectors drew the same level of leakage current up to 500 V. The saturation bias voltage of the leakage currents seemed to be about 300 V for all three detectors.

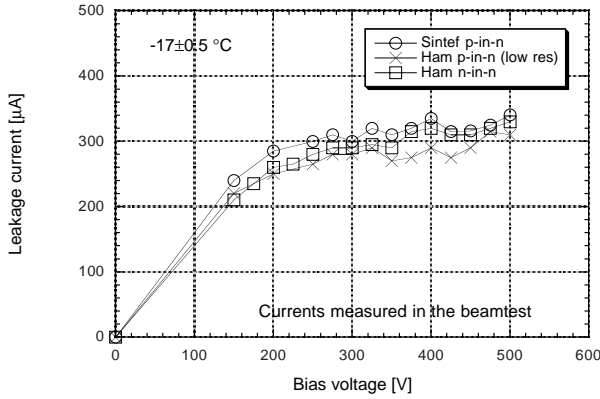


Figure 5: Leakage currents of the radiation-damaged detectors during the beamtest. Environment temperature was set at -17°C .

C. Charge collection

With one threshold in the electronics, only efficiency of detecting signals above the threshold in a single strip was obtained at a time. By scanning the thresholds, the pulse height distribution, so-called Landau distribution, was obtained as its integral form. An example of the threshold scan is shown in Figure 6.

The median of the Landau distribution was the threshold of 50% efficiency. In order to get the threshold, a modified error function, eq. (1), was fitted to the efficiency data.

$$\text{eff}(q) = p_3 \cdot \left(1 - \text{erf} \left(\frac{q - p_1}{p_2} f(q) \right) \right) \quad (1)$$

where

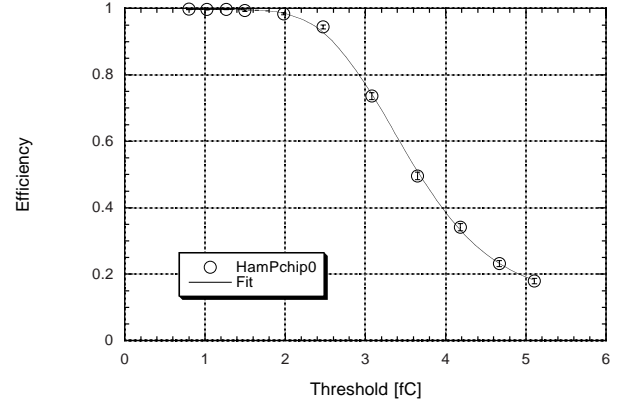


Figure 6: An example of threshold scan for a channel in the Hamamatsu p-in-n detector. The efficiency curve was fit to a function described in the text and the median charge was defined at the threshold of 50% efficiency.

$$f(q) = \max \left(0.6, 1 - p_4 \left(\frac{q - p_1}{p_2} \right) \right) \quad (2)$$

The function, erf , was the integral of the Gaussian distribution. The function, $f(q)$, was a phenomenological correction function to modify the Gaussian to the Landau distribution. The fitting parameters expressed the median (p_1), the width (p_2), the saturation (p_3), and the skew (p_4).

The median charges were shown as a function of bias voltages in Figure 7. A number of corrections were involved to reach this figure: (1) The median charges of each LBIC chips were scaled so that the average of the medians in the "strip region" at the bias voltages of 450, 475, and 500 V to be 3.5 fC. This was to correct the non-uniform radiation-damage within a detector, and also correct the imperfect calibration of the amplifier responses. The definition of the "strip region" will be given in the section D; (2) The bias voltages were corrected for the leakage current to give the bias voltages applied to the silicon bulk. There was a resistance of 11 k Ω in the bias power supply line externally; and (3) The bias voltages of the Sintef p-in-n detector were increased to correct the thickness by a simple theoretical expectation of $(300 \mu\text{m}/293 \mu\text{m})^2$ which was to increase the bias voltages by 4.8%.

The data showed: (1) the p-in-n detectors required higher voltages to reach the same median charges of the n-in-n detector, and (2) two p-in-n detectors collected charges very similarly.

The first observation was the reflection of the location of the p-n junction after the type inversion: the p-n junction of the p-in-n detector was in the backside, while that of the n-in-n detector was in the strip side. The charge signals were induced in the strips when the real charges moved along the electric field. In the p-in-n detector, the high electric field was near the backside which was several times the strip pitch away from the strips. The charge signals might have been split into several strips. In the n-in-n detector, the highest electric field was near the strips and the charge signals were induced only one strip nearby. A

circumstantial evidence was also obtained in the ratios of the median charges in the inter-strip over the strip regions in the section D.

Since the n-in-n detector after the type inversion had the p-n junction in the readout side, the charge collection could be compared with the ideal diode, where the collected charges scales as the depletion depth, $V^{-0.5}$, and saturated once fully depleted. This ideal charge collection was plotted on the Figure 7 with the full depletion voltage being set at 300 V. The charge collection of the n-in-n detector was close to the ideal diode but slightly different, which could be caused by the strip structure of the electrodes and by the binary readout electronics.

The second observation indicated that there was very little difference in the charge collection in the low and the high resistivity wafers, after the fluence in this test. Providing that the charge collection was reflecting the depletion depth and the fundamental property of the p-in-n detectors from two vendors was equal, there would be little difference in the full depletion voltages of the two wafers.

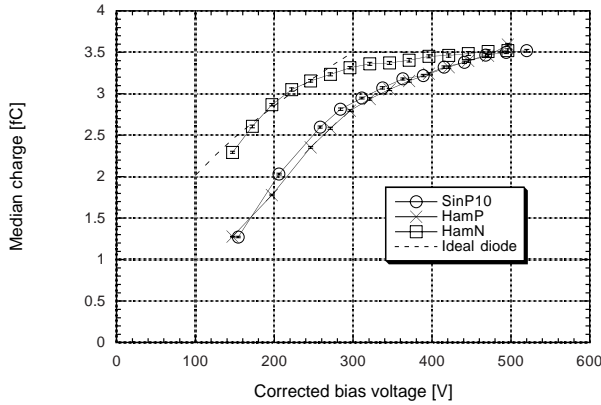


Figure 7: Median charges of the radiation-damaged detectors as a function of bias voltages. The “ideal diode” is the theoretical expectation of the collected charges which scales as \sqrt{V} and saturates at 300 V.

D. Charge collection in the inter-strip region

Electrons and holes liberated in the Silicon bulk will travel along the electric field lines. The charges moving the midway between the strips induce charges in the two neighbour strips equally, i.e., the charges split into two strips.

The median charges were classified according to the beam particle positions. The positions around the midway between the strips with a width of 20 μm was defined as the inter-strip region. The positions around the strips with a width of 40 μm was defined as the strip region. The ratios of the median charges in the inter-strip over the strip regions are shown in Figure 8. Since the ratio was taken, the uncertainties associated with the non-uniform damage, imperfect calibration, etc. were eliminated.

The ratios of the n-in-n detector were insensitive to the bias

voltage, while those of the p-in-n detectors were distinctively different: the ratio was much lower in the low bias voltages and increased as the bias voltage increased to the level of the n-in-n detector near the highest voltages. This would be another indication that more charges were split into strips in the p-in-n detectors.

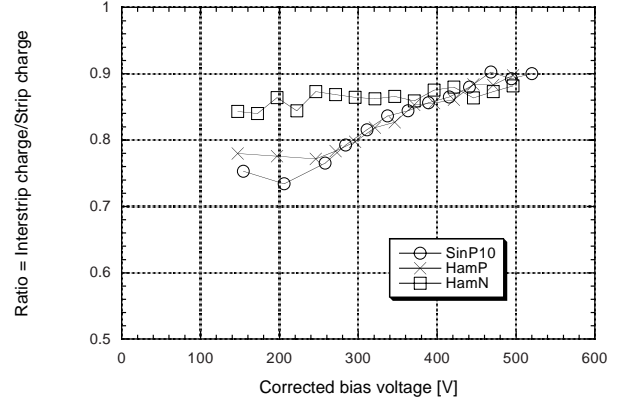


Figure 8: Ratios of the median charges in the inter-strip and the strip regions as a function of the bias voltages. The inter-strip region was defined in the midway between the strips with a width of 20 μm , and the strip region around the strips with a width of 40 μm .

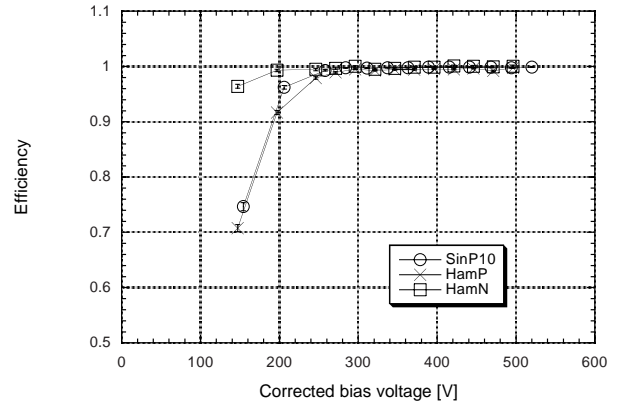


Figure 9: Bias voltage dependence of the efficiency at the threshold of 1 fC.

E. Efficiency at 1 fC

In a real experiment, the data taking will be made by setting the threshold at one point. From the efficiency and electronics noise argument, the threshold is to be set around 1 fC. The bias voltage dependence of the efficiency at a threshold of 1 fC is shown in Figure 9. The p-in-n detectors, although required larger bias voltages than the n-in-n detector, became efficient (>99%) above the bias voltage of 250 V.

V. SUMMARY

Two p-in-n and one n-in-n Silicon microstrip detectors of the ATLAS Silicon microstrip detector specification were radiation-damaged and beamtested. Two comparisons: comparison of p-in-n and n-in-n detectors, and low and high resistivity wafers motivated the study. The resistivity of the wafers were 1 k Ω cm for the low resistivity and 4 or 5 k Ω cm for the high resistivity wafers. The proton fluence was 4.2×10^{14} p/cm². The detectors were kept cold during the irradiation and stored cold.

Prior to the beamtest, the damaged detectors were warmed up to anneal and to include the warm-up in the maintenance in the real experiment. Although the body capacitances implied that the low resistivity wafer had a lower corner voltage, the voltage was not a clear evidence of a lower full-depletion voltage.

In the beamtest, the detectors were read out with a fast-shaping one-threshold electronics. By scanning the threshold, the charge collection information in a single strip was obtained. The median charges showed that the full-depletion voltage would be around 300 V in the n-in-n detector. The leakage currents suggested all three detectors had the similar full-depletion voltage around 300 V.

There was no clear saturation in the median charges in the p-in-n detectors. The p-in-n detectors required larger bias voltages (by 70~100V) to reach the same median charges of the n-in-n detector. The ratios of the median charges in the interstrip over the strip regions showed larger charge loss in the p-in-n detectors in low bias voltages. These observations would suggest that the charges were split into several strips in the p-in-n detectors.

The two p-in-n detectors, low and high resistivity wafers, behaved very similarly. Although the full-depletion voltages of the two detectors were not evident in the charge collection, the similarity suggested that there was little difference in the full-depletion voltages of the different resistivity wafers, providing the fundamental character of the detectors from the two manufacturers was the same.

The p-in-n detectors required more bias voltages to collect charges, however, the efficiency at 1 fC showed that the detectors were efficient once the bias voltage was over 300 V.

VI. ACKNOWLEDGEMENT

The authors wish to acknowledge the cooperation of the beam channel crews of the EP1A and π 2 beamline of the KEK PS for the irradiation and the beamtest. This work was supported by Japan Ministry of Education, Science, and Culture, Japan Society for Promotion of Science, Australian Research Council, and UK Particle Physics and Astronomy Research Council.

VII. REFERENCES

- [1] ATLAS Inner Detector Technical Design Report, CERN/LHCC/97-17, ATLAS TDR 5, 30 April 1997
- [2] T. Ohsugi et al., "Micro-discharge noise and radiation damage of silicon microstrip sensors", Nucl. Instr. Metho. A383, pp. 166-173, 1996
- [3] Y. Unno et al., "Characterization of an Irradiated Double-sided Silicon Strip Detector with Fast Binary Readout Electronics in a Pion Beam", IEEE Trans. Nucl. Scie., Vol. 43, pp. 1175-1179, 1996
- [4] Y. Unno et al., "Beam Test of a Large Area N-on-n Silicon Strip Detector with Fast Binary Readout Electronics", IEEE Trans. Nucl. Scie., Vol. 44, pp. 736-742, 1997; Y. Unno et al., "Evaluation of P-stop Structures in the N-side of N-on-n Silicon Strip Detector", IEEE Trans. Nucl. Scie., Vol. 45, pp. 401-405, 1998
- [5] D. Pitzl et al., "Type inversion in silicon detectors", Nucl. Instr. Metho. A311, pp. 98-104, 1992
- [6] SINTEF Electronics and Cybernetics, P. O. Box 124 Blindern, N-0314 Oslo, Norway
- [7] Hamamatsu Photonics, 1126-1, Ichino-cho, Hamamatsu-shi 435, Japan
- [8] S. Terada et al., "Proton irradiation on silicon detectors and related materials", T363, KEK test experiment
- [9] S. Terada et al., "Proton irradiation on p-bulk silicon strip detectors using 12 GeV PS at KEK", Nucl. Instr. Metho. A383, pp. 159-165, 1996
- [10] H.-J. Ziock et al., "Temperature dependence of the radiation induced change of depletion voltage in silicon PIN detectors", Nucl. Instr. Metho. A342, pp. 96-104, 1994
- [11] Y. Unno et al., "Beamtest of the radiation-damaged silicon microstrip detectors", T429, KEK test experiment
- [12] LBIC: E. Spencer et al., "A Fast Shaping Low Power Amplifier-Comparator Integrated Circuit for Silicon Strip Detectors", IEEE Trans. Nucl. Scie., Vol. 42, pp. 796-802, 1995; CDP: J. DeWitt, "A Pipeline and Bus Interface Chip for Silicon Strip Detector Read-out", Proc. IEEE Nucl. Scie. Symp., San Francisco, CA., Nov. 1993
- [13] O. Toker, S. Masciocchi, E. Nygard, A. Rudge, P. Weilhammer, "Viking: A CMOS low noise monolithic 128-channel frontend for Si strip detector readout", Nucl. Instr. Metho. A340, pp. 572-579, 1994
- [14] Particle Data Group, "Review of Particle Physics", Eur. Phys. J. C3, pp. 146, 1998